Bennett, A.G. and Rabbetts, R.B. *Clinical Visual Optics, 2nd ed.* (Butterworth-Heinemann Ltd., London, 1989).

# 2

# The eye's optical system

## The eye and the camera

Considered as an optical instrument, the eye has certain similarities to a camera, though it would be truer to say that the camera has been copied from the eye. The points of difference are worth noting, the eye being superior on almost every count. It is much more compact, has a wider field of view, operates over a much more extensive range of luminance levels and its resolving power is close to the theoretical limit. Paradoxically – as Helmholtz pointed out – the typical eye nevertheless exhibits aberrations and errors of centration that an optical designer would consider unacceptable in a high-grade man-made system.

The aberrations of the eye are considered in detail in Chapter 15 and so here we shall look at the basic image-forming properties of the eye from the standpoint of simple geometrical optics valid for the paraxial region. Although you are probably familiar with optical principles, an outline of the notation and methods used in this book is given in the following pages. For a more detailed treatment including proofs, the works listed in the bibliography at the end of the book are useful.

## Laws of optical image formation

### Sign convention

(1) Distances measured in the same direction as that in which the incident light is travelling are regarded as positive in sign; if in the opposite direction, as negative.

(2) Object and image distances, focal lengths and radii of curvature are measured *from* the lens, mirror or surface concerned. The sign follows from (1).

(3) Diagrams are normally drawn so that the incident light travels from left to right.

(4) The vertical distance from the optical axis to a point above it is taken as positive, and to a point below it as negative.

(5) For some purposes, a sign convention for angles is needed. In accordance with accepted mathematical convention, angles measured in an anti-clockwise direction are regarded as positive. The angle between a ray and the optical axis is measured from the ray to the axis.

### Symbols

Standard symbols for the most important quantities are as follows:

| | |
|---|---|
| Refractive index | $n$ |
| Object distance | $\ell$ |
| Image distance | $\ell'$ |
| First focal length | $f$ |
| Second focal length | $f'$ |
| Radius of curvature | $r$ |
| Object height | $h$ |
| Image height | $h'$ |

The presence of a dash (or 'prime') shows at once that the symbol refers to a quantity after refraction or reflection, the same symbol undashed denoting the corresponding quantity before refraction or reflection.

To denote the reciprocal of a distance, the corresponding capital letter is used. Thus $L = 1/\ell$, $R = 1/r$ and so on.

Letters used as symbols denoting a quantity are normally printed in italic type. On the other hand, letters in Roman capitals denote geometrical points. This helps to distinguish between $F$ (the power of a lens or surface) and F (the first principal focus).

Subscript numerals are helpful in identifying one of a series of successive refractions or reflections. For example $h_2'$ denotes the image height after the second refraction or reflection.

## 'Real' and 'virtual'

When refraction or reflection takes place at two or more surfaces in succession, the image formed at the first, whatever its nature, becomes the object for the next. This gives rise to the possibility of 'virtual' objects as well as virtual images. Real and virtual types of object may give rise to either type of image.

### *Definitions*

(1) A real object is one from which incident rays diverge.
(2) A virtual object is one towards which incident rays are converging as the result of a previous refraction or reflection.
(3) A real image is one towards which refracted or reflected rays converge and is therefore capable of being received on a screen.
(4) A virtual image is one from which refracted or reflected rays *appear* to emanate.

## Refraction at a spherical surface

Let A be the vertex and C the centre of curvature of a spherical surface, a line through A and C being taken as the 'axis' (*Figure 2.1*).

If the surface is converging (for example, convex, air to glass) the first principal focus F is the real point on the axis giving rise to an image at infinity, the refracted ray being parallel to the axis. The second principal focus F′ is the real image point on the axis corresponding to an object point at infinity, the incident rays being parallel to the axis.

The same definitions apply to a diverging surface, except that in this case F is a virtual object point and F′ a virtual image point (*Figure 2.2*).

In both cases, the distance AF is the first focal length $f$ and AF′ the second focal length $f'$.

Let B be an axial object point giving rise to the image point B′ (*Figure 2.3*). Then, in all possible cases,

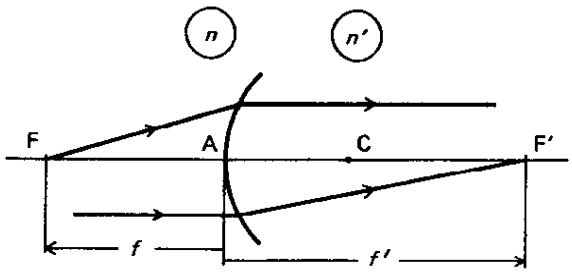


**Figure 2.1.** Principal foci F and F′ of a converging spherical refracting surface.

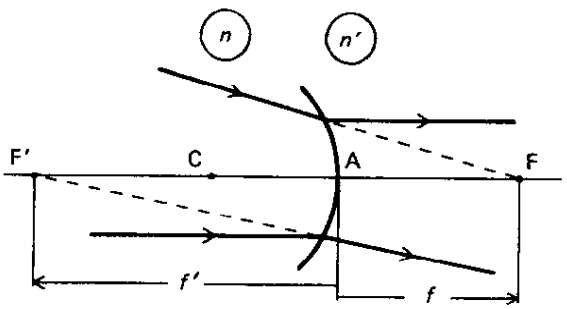


**Figure 2.2.** Principal foci F and F′ of a diverging spherical refracting surface.

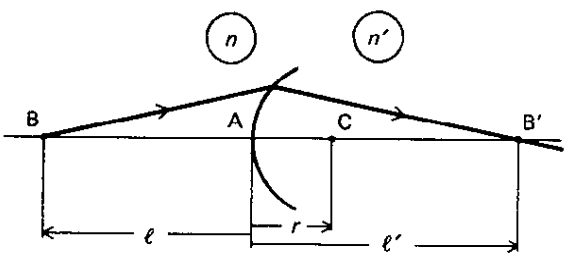


**Figure 2.3.** Refraction at a converging spherical surface.

$\ell$ = AB
$\ell'$ = AB′
$r$ = AC
$n$ = refractive index of first medium
$n'$ = refractive index of second medium

and

$$\frac{n'}{\ell'} = \frac{n}{\ell} + \frac{n' - n}{r} \qquad (2.1)$$

For an object at infinity, $n/\ell = 0$ and $\ell' = f'$. Similarly, for an image at infinity $n'/\ell' = 0$ and $\ell = f$. Hence

$$\frac{n'}{f'} = \frac{-n}{f} = \frac{n' - n}{r} \qquad (2.2)$$

## Power and vergence

For a spherical refracting surface, the power $F$ is given by the relationship

$$F = \frac{n'}{f'} = \frac{-n}{f} = \frac{n' - n}{r} = (n' - n)R \qquad (2.3)$$

where the curvature $R$ is the reciprocal of the radius of curvature in metres. The unit of curvature is the reciprocal metre ($m^{-1}$). From equation (2.3) the surface power is seen to be proportional to the *reciprocal* of the focal lengths. The unit of focal power is the dioptre (D), the focal lengths being expressed in metres for this purpose.

The term 'reduced distance' denotes a distance (or thickness of material) traversed by a pencil of rays, divided by the refractive index of the given medium. On this basis, the reciprocal of a reduced object or image distance, such as $n'/\ell'$ in equation (2.1), is traditionally called the 'reduced vergence'. For brevity, however, we shall omit the word 'reduced' from this term. In this work, vergence will be used to denote the reciprocal of an object or image distance (in metres) multiplied by the refractive index of the corresponding medium.* Like focal power, its unit is the dioptre. Accordingly

Object vergence $L = n/\ell$ (in metres)
Image vergence $L' = n'/\ell'$ (in metres)

* The term vergence has traditionally been used as a synonym for wavefront curvature, the unit of which is the reciprocal metre, not the dioptre.

Equation (2.1) can now be re-written in the more convenient form

$$L' = L + F \qquad (2.4)$$

in which all quantities are in dioptres.

It is a fundamental rule that a positive value of $L$ or $L'$ always denotes convergence, while a negative value always denotes divergence.

Unless otherwise stated, all distances in algebraic formulae throughout this book should be taken to be in metres. If numerical values in millimetres are substituted in such expressions, a compensating factor of 1000 must be introduced.

## The thin lens

A thin lens in air has two principal foci F and F′ and two focal lengths $f$ and $f'$, defined exactly as for a spherical refracting surface. In this case, however, the power $F$ of the lens is given by

$$F = 1/f' = -1/f \qquad (2.5)$$

again in dioptres if $f'$ and $f$ are in metres.

The conjugate focus relationship (2.4) applies equally to a thin lens in air.

## Reflection

When light is reflected by a mirror (*Figure 2.4*) whether plane or spherical, there is a reversal of direction which upsets the usual correspondence between the signs of $\ell'$ and $L'$. The same applies to the focal length of a mirror since the focal length is also an image distance. Consequently, for reflection only we must put (assuming the mirror is in air)

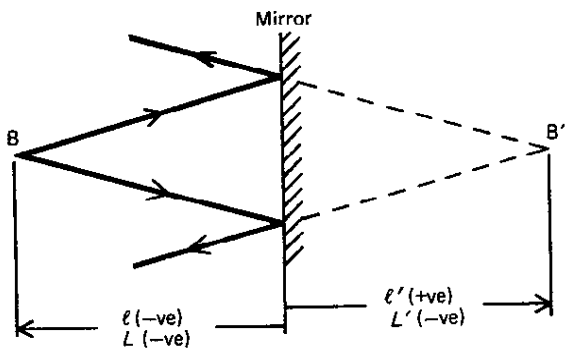


**Figure 2.4.** Sign convention for reflection.

$$L' = -1/\ell'; \qquad \ell' = -1/L' \quad (2.6)$$

and

$$F = -1/f' = \frac{-2}{r}; \qquad f' = -1/F \quad (2.7)$$

There is, however, no change in the relationship $L = 1/\ell$.

The conjugate focus relationship for reflection then assumes the familiar form

$$L' = L + F$$

Theoretically, reflection obeys the same laws as refraction if $-n$ is substituted for $n'$.

## Unequifocal systems

The eye is an example of an unequifocal optical system, one in which the first and last media have different refractive indices. In general, such systems have six cardinal points (*Figure 2.5*) as follows:

(1) F and F′, the first and second principal foci, defined exactly as for a single refracting surface.
(2) P and P′, the first and second principal points.
(3) N and N′, the first and second nodal points.

The cardinal points are always symmetrically positioned such that PP′ = NN′ and FP = N′F′.

The system as a whole has an 'equivalent power' $F$ such that

$$F = \frac{n_{k+1}}{f'} = \frac{-n_1}{f} \quad (2.8)$$

where $f'$ = P′F′, $f$ = PF, $n_1$ = refractive index of first medium and $n_{k+1}$ = refractive index of last medium, the system having $k$ surfaces.

If the object distance $\ell$ is measured from P and the image distance $\ell'$ is measured from P′, the conjugate focus relationship again takes the form

$$L' = L + F$$

where $L = n_1/\ell$ and $L' = n_{k+1}/\ell'$.

Let a ray from an extra-axial object point Q be directed towards P, making an angle $u$ with the optical axis (*Figure 2.6*). The corresponding emergent ray will appear to have passed through P′ making an angle $u'$ with the optical axis such that

$$n_{k+1}u' = n_1u \quad (2.9)$$

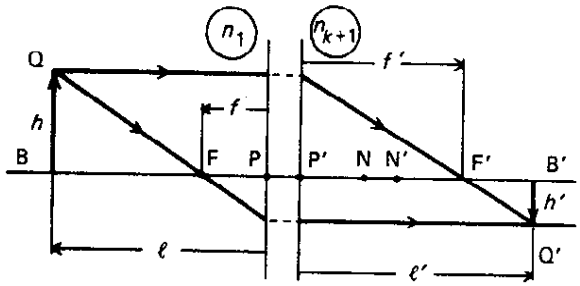


**Figure 2.5.** The cardinal points and conjugate foci of an unequifocal refracting system.

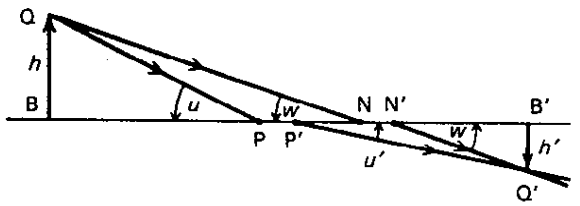


**Figure 2.6.** Image construction for an optical system using the principal and nodal points.

Let another ray from Q be directed towards the first nodal point N. The corresponding emergent ray will appear to have passed through the second nodal point N′ without undergoing a change of direction. As indicated in *Figure 2.6*, these two pairs of rays can be used to construct the image B′Q′ of an object BQ.

The properties of the two principal foci F and F′ can also be used for this purpose, as shown in *Figure 2.5*.

## Transverse magnification

The expression

$$m = h'/h = L/L' \quad (2.10)$$

in which $m$ denotes the transverse magnification, applies equally to refraction and reflection at a single surface, as well as to thin lenses and optical systems. Because this vergence formula for magnification is so general, its use is preferable to the alternative forms, in which vergence is expressed in terms of object and image distances.

## Effectivity

Let a pencil of rays (*Figure 2.7*) be travelling in a medium of refractive index $n$ and let the distance

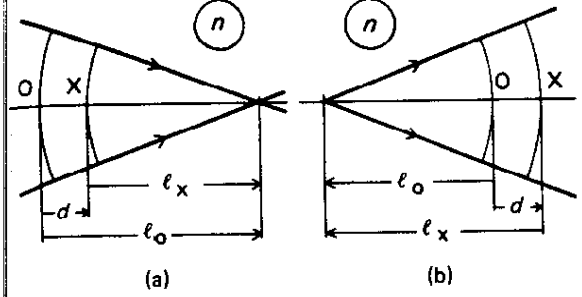


**Figure 2.7.** Effectivity: (a) converging bundle, (b) diverging bundle.

to the origin (or from the focus) of the pencil be $\ell_o$ measured at a specific point O. After travelling a distance $d$ metres from O to another specified point X, the wavefront is at a distance $\ell_x$ from its origin or focus. Hence,

$$\ell_x = \ell_o - d$$

and

$$L_x = \frac{n}{\ell_x} = \frac{n}{\ell_o - d} = \frac{n}{(n/L_o) - d}$$

$$= \frac{L_o}{1 - (d/n)\, L_o} \qquad (2.11)$$

This expresses a general effectivity relationship, 'effectivity' denoting a change of vergence as light passes from one surface or reference point to another.

If $d$ is relatively small, the above expression can be expanded by the binomial theorem to give the useful approximation

$$L_x \approx L_o\left(1 + \frac{d}{n}L_o + \ldots\right)$$

$$\approx L_o + \frac{d}{n}.L_o^2 + \ldots \qquad (2.12)$$

The quantity $d/n$ is an example of a reduced distance.

### Refractive index

The refractive index of a transparent medium varies with wavelength, and, to a lesser extent, with temperature. Unless the context indicates otherwise, the term should be understood as an abbreviation for 'mean refractive index', namely, the value for a selected wavelength in the brightest part of the spectrum. The d-line of the helium spectrum ($\lambda$ = 587.6 nm) is often chosen for this purpose. Measurements are normally made at a temperature in the neighbourhood of 18 to 20 °C.

### Angles and prism power

Throughout the text, angles will be expressed in radians, degrees, or prism dioptres (symbol Δ). This last measure, which is of great convenience in ophthalmic optics, was introduced in 1890 by C. F. Prentice (but not given this name by him).

If $u$ is any angle less than 90°, then

$$u \text{ in } \Delta = 100 \tan u \qquad (2.13)$$

Thus, in *Figure 2.6*

$$u = 100(\mathrm{BQ/BP})\ \Delta$$

A disadvantage of this system is that the tangent of an angle does not increase in proportion to the angle itself when other than small values are concerned. For example, 20 Δ is equivalent to $\tan^{-1}$ 0.20 or 11.31°, whereas 40 Δ is equivalent to $\tan^{-1}$ 0.40 or 21.80°.

For small angles, the formula

$$4^\circ = 7\,\Delta \qquad (2.14)$$

is an easily remembered and useful approximation.

It also follows from equation (2.13) that for small values the prism dioptre is equivalent to one-hundredth of a radian, since both the sine and the tangent of a small angle are very nearly equal to the angle itself in radian measure.

In the ophthalmic world, the prism dioptre is the accepted unit of prismatic power and deviation. According to the currrent British Standard* for ophthalmic trial case lenses, prisms are to be numbered according to the deviation (in Δ) undergone by a ray of wavelength 587.6 nm incident normally at one surface.

## The cornea

With this introduction we can now study the various components of the eye's optical system, first in sequence and then the system as a whole.

---

* BS 3162: 'Ophthalmic Trial Case Lenses'.

The cornea (*Figure 2.8*) is a highly transparent structure of meniscus form, approximately 12 mm in diameter and slightly smaller vertically than horizontally. The centre thickness is usually between 0.5 and 0.6 mm.

A thin layer of lacrimal fluid normally covers the anterior surface but it is too thin to affect the power appreciably and may be ignored in this context.

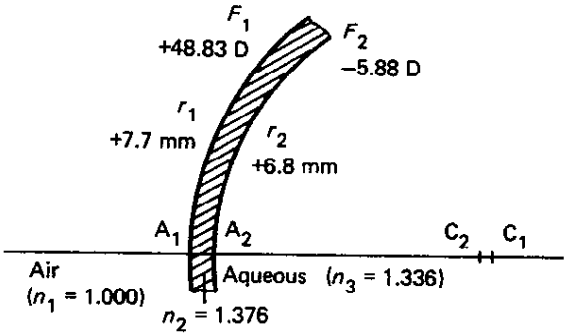


**Figure 2.8.** Profile of the human cornea (to scale): average values as adopted in Gullstrand's schematic eye.

To a first approximation both surfaces may be regarded as spherical, the radii of curvature having values in the neighbourhood of +7.7 mm (anterior) and +6.8 mm (posterior).*

The refractive index of the corneal substance may be taken as 1.376 and that of the aqueous humour, in contact with the back surface of the cornea, as 1.336.* By applying equation (2.3), the two surface powers of the cornea may be found as follows:

(1) *Anterior surface*

$$\text{Power } F_1 = \frac{1000\,(1.376 - 1)}{+\,7.7}$$

$$= +\,48.83 \text{ D}$$

(2) *Posterior surface*

$$\text{Power } F_2 = \frac{1000\,(1.336 - 1.376)}{+\,6.8}$$

$$= -5.88 \text{ D}$$

The power of the cornea as a whole is therefore about +43 D, over two-thirds of the total power of the eye.

* The values assumed by Gullstrand in his schematic eye.

When the eyes are unprotected under water, the anterior surface of the cornea has its power greatly reduced, the retinal image then becoming inordinately blurred.

## The anterior chamber

The anterior chamber is the cavity lying behind the cornea and in front of the iris and crystalline lens. It is filled with a colourless liquid aptly termed the aqueous humour since its water content is 98%.

The depth of the anterior chamber, measured along the eye's optical axis, is strictly the distance from the posterior vertex of the cornea to the anterior surface of the crystalline, but the term as sometimes used includes the corneal thickness. Excluding this latter, an average value would be about 3.0 mm.

From an optical point of view, the depth of the anterior chamber is important inasmuch as it affects the total power of the eye's optical system. If all other elements remained unchanged, a reduction of 1 mm in the depth of the anterior chamber (through a forward shift of the crystalline) would increase the eye's total power by about 1.4 D. The reverse effect would result from a shift in the opposite direction.

## The iris and pupil

The amount of light admitted to the eye is regulated by the pupil, an approximately circular opening in the iris.

In normal conditions the pupils react to:

(1) A change in luminance–the 'direct' reflex
(2) A change in luminance applied to one eye only, also producing a 'consensual' reflex in the fellow eye,
(3) Near fixation, which is accompanied by pupillary contraction.

Failure or anomaly of one or more of these reflexes may be an important pointer to some underlying disorder.

The pupil size decreases with age at an approximately uniform rate which does, however, tend to slow down in later life. Largely because of differences in techniques of measurement, there is only a limited measure of agreement between various published studies. The following diameters can be taken as typical. For the eye in total

darkness, 7.6 mm at age 10, 6.2 mm at age 45, and 5.2 mm at age 80. For the light-adapted eye, 4.8 mm at age 10, 4.0 mm at age 45, and 3.4 mm at age 80.

Pupil size can be affected by a number of external or secondary agencies such as drugs, emotions, and sudden changes in the state of mind.

## The crystalline lens

The crystalline lens serves the double purpose of supplying the balance of the eye's refractive power and providing a mechanism for focusing at different distances. This latter faculty is called accommodation.

Both anatomically and optically, the lens is a highly complex structure, composed of layers of fibres laid down in an essentially radial pattern that is regular enough to allow a symmetrical diffraction halo to be formed (*see* Chapter 22). The lens continues to grow in bulk throughout life by the formation of fresh layers of fibres on the exterior. As part of the normal process of ageing it is susceptible to various changes impairing its flexibility and transparency. Its centre thickness is thereby increased, while the radii of curvature may become longer.

The lens substance is enclosed in a highly elastic capsule. A structure of suspensory ligaments, called the zonule of Zinn, stretches from the periphery of the capsule to the surrounding ciliary body, holding the lens in position and controlling the curvature of its surfaces through variations in tension produced by the action of the ciliary muscle.

The lens has a diameter of approximately 9 mm and is biconvex in form, the radius of its anterior surface being about 1.7 times that of its posterior surface. When the lens is in its unaccommodated state, the centre thickness has traditionally been taken as 3.6 mm, a figure appropriate to a young adult. As accommodation is brought into play, both surfaces, but especially the anterior, assume a more steeply curved form. The centre thickness thus increases and the vertex of the anterior surface moves forward, reducing the depth of the anterior diameter. The profiles of a typical crystalline in its relaxed and fully accommodated states are shown superimposed in *Figure 2.9* which has been drawn to scale. The diagram also indicates the range of positions of the two centres of curvature.

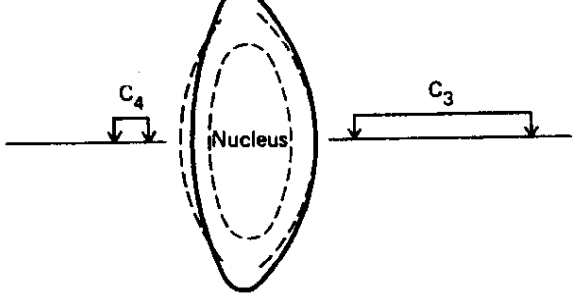


**Figure 2.9.** Profiles of the human crystalline lens in its relaxed and fully accommodated states.

The back surface of the crystalline is in contact with the vitreous humour, a transparent gel which fills the posterior segment of the globe. The vitreous humour has very nearly the same chemical composition as the aqueous and its refractive index may be taken as the same, 1.336.

Because of its onion-like structure and the compression exerted on the innermost layers, the crystalline lens is far from being optically homogeneous. A slit-lamp section reveals several bands of discontinuity. In particular, it is possible to distinguish a central bi-convex portion called the nucleus, from the surrounding portion, called the cortex. In the centre of the nucleus, the refractive index reaches its maximum value between 1.40 and 1.41 but diminishes from the centre outwards, being about 1.385 near the poles and about 1.375 near the equator.

It may easily be deduced that a refractive index gradient of this pattern, irrespective of any surface curvatures, must produce a converging effect like a positive lens. Since the velocity of light in a medium is inversely proportional to its refractive index, an incident wavefront would become progressively less retarded from the centre outwards and hence assume a convergent form. By way of confirmation, Ivanoff (1953) crushed a rabbit crystalline between parallel glass plates so that all the surfaces including those of the nucleus were rendered effectively plane. He then found that the element so produced had a power in air of just over +6 D.

In his book on *Physical Optics*, Wood (1911) described a simple method of making 'pseudo lenses' from discs of gelatine enclosed between glass plates. Immersion in water, which has a lower refractive index, brings about a progressive decline in index towards the periphery, producing positive power up to about +12 D. Both Ivanoff

(following Bouasse) and Wood have given mathematical analyses.

As a result of this effect, the crystalline lens has a greater power than would be the case if its refractive index were uniform and had the highest value actually found. In fact, it is necessary to assume a fictitious refractive index of about 1.42 to bring the power of a homogeneous crystalline lens up to a typical value in the neighbourhood of +21 D.

The assumption that the lens surfaces are spherical is for convenience only. Careful observation reveals a marked degree of peripheral flattening, especially of the anterior surface in its accommodated state. Owing to this, and to the peripheral flattening of the cornea, the eye's spherical aberration is kept within reasonable limits, as we shall see in Chapter 15.

## The retina

Anatomically an outgrowth of the brain, the retina is a thin but enormously intricate structure, its functions being much more extensive than was originally supposed. It lines the posterior portion of the globe, extending functionally up to the *ora serrata* close to the ciliary body.

A surprising feature of the retina is that the nerve fibres transmitting impulses from individual or groups of retinal receptors travel across its surface to their exit via the main trunk of the optic nerve. The retina is also supplied with blood vessels which are clearly visible through an ophthalmoscope. Despite these obstructions to the incident light, the efficiency of the system does not appear to suffer. Under certain conditions, however, retinal blood vessels may be seen entoptically by the shadows which they cast (*see* Chapter 22).

As described more fully in Chapter 3, the ability of the retina to distinguish detail is not uniform over its entire extent and reaches a maximum in the macular region. This is an approximately circular area of diameter about 1.5 mm containing a smaller central area, the fovea, populated exclusively by retinal cones. It is at the fovea that the eye attains its maximum resolving power. When an object engages visual attention, the two eyes are instinctively turned so that the image lies on each fovea.

From an optical point of view, the retina could be described as the screen on which the image is formed. It can be regarded as part of a concave spherical surface with a radius of curvature in the neighbourhood of −12 mm.

In cameras and optical instruments generally, it is convenient to have images formed on plane surfaces, but the curvature of the retina has two positive advantages. In the first place, the images formed by optical systems tend to have curved surfaces. The curvature of the retina is of the right order from this point of view (*see* Chapter 15). Secondly, the steeply curved retina is able to cover a much wider field of view than would otherwise be possible.

## The schematic eye

### General properties

The schematic eye is a theoretical optical specification of an idealized eye, retaining average dimensions but omitting the complications (*see* Chapter 12 for details). The equivalent power of the eye as a whole is about +60 D and its cardinal points are situated as shown in *Figure 2.10*. The first and second principal points, P and P′, lie in the anterior chamber at distances of about 1.6 and 1.9 mm respectively from the front surface of

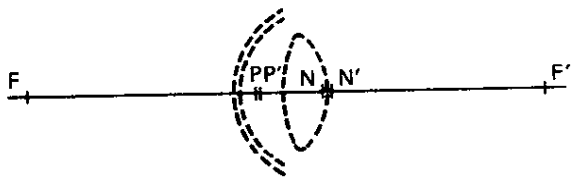


**Figure 2.10.** The cardinal points of the unaccommodated schematic eye (to scale).

the cornea. The nodal points, N and N′, are also separated by 0.3 mm and straddle the back surface of the crystalline lens. The anterior focal length PF is about −16.7 mm and the posterior focal length P′F′ about +22.2 mm.

The general relationships and ray paths indicated in *Figures 2.5* and *2.6* apply in every particular to the schematic eye.

### Optical centration

In the schematic eye it is assumed that all the refracting surfaces are co-axial, the cornea and

crystalline having a common optical axis. The optical centration of the typical human eye seems to be defective, the crystalline lens being usually decentred and tilted with respect to the cornea. For this reason the eye does not possess a true optical axis. However, as shown in Chapter 12, the principal points of the cornea very nearly coincide as do those of the schematic crystalline lens. Consequently, a line drawn as nearly as possible through these two pairs of points would represent a very close approximation to an optical axis. The use of this term in relation to the eye can be justified on this basis.

## Entrance and exit pupils

If a pupil HJ (*Figure 2.11*) with its centre at $E_o$ is regarded as an object for the cornea, it will give rise to a slightly magnified image with its centre at E. This image is called the 'entrance pupil'. Taken as an object for the crystalline lens, the pupil HJ will give rise to another image, the 'exit pupil', with its centre at E'.

It follows from this that an incident pencil of rays directed towards and filling the entrance pupil would pass through the entire area of the real pupil, after refraction by the cornea, and on finally emerging into the vitreous body, would appear to have been limited by the exit pupil.

Further, since a ray directed towards the axial point E appears after refraction to have passed through the axial point E', these two points must be conjugate with respect to the system as a whole.

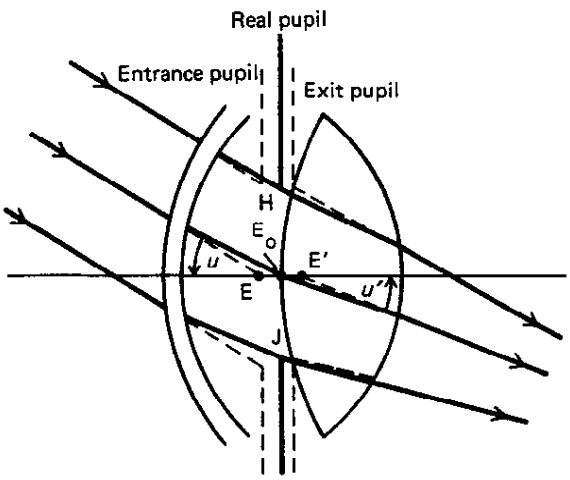


**Figure 2.11.** The eye's real pupil and its images, the entrance and exit pupils.

On the basis of paraxial theory, it may be shown that the entrance pupil is situated about 3 mm behind the anterior surface of the cornea and is about 13% larger than the real pupil. The exit pupil lies closely behind the real pupil and is only 3% larger.

Because E and E' are conjugate points, another relationship can be established. If an incident ray directed towards E makes an angle $u$ with the optical axis, the conjugate refracted ray will make an angle $u'$ with the axis such that

$u'/u$ = a constant for a given system

For the schematic eye the value of this constant is about 0.82.

## The visual axis

It might be reasonable to expect that the fovea would be situated on the retina at its intersection with the optical axis, a point termed the 'posterior pole'. In fact, the fovea is normally displaced temporally and downwards from the expected position. We are therefore led to postulate a 'visual axis' as distinct from the optical axis.

The visual axis has been taken by many writers to be the imaginary line directed towards the first nodal point N such that a parallel line through N' would pass through the fovea. Apart from a slight displacement due to the separation of the two nodal points, as seen in *Figure 2.6*, an incident ray travelling along this path would be otherwise undeviated. Indeed, it could be assumed without serious error that a mean position of the two nodal points existed and the visual axis could be defined as the line passing through this mean position and the fovea.

However, the present writers share the objection to this concept already voiced by others. The term 'visual axis' ought to mean the axis or chief ray of the actual pencil of rays which enters the pupil and is converged to the fovea. Accordingly, despite the weight of present contrary opinion, the term 'visual axis' will be used here to denote the incident ray path directed towards the centre E of the entrance pupil such that the conjugate refracted ray falls on the fovea, M' (*Figure 2.12*).

The angle between the optical and visual axis is called the angle alpha, and is considered positive when the visual axis in object space lies on the

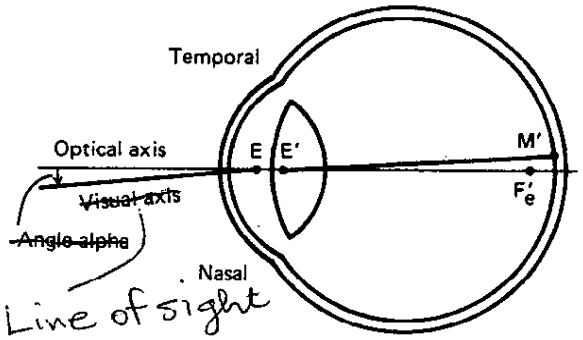


**Figure 2.12.** The optical and visual axes of the eye. Its second principal focus $F'_e$ is shown in a position indicating myopia.

nasal side of the optical axis. A positive value in the neighbourhood of 5° is commonly found. There seems to be general agreement with Donders' observation that the angle tends to be smaller in myopia and greater in hypermetropia.

As for the vertical plane, the visual axis in object space is generally inclined in an upward direction from the optical axis, the figure commonly quoted being about 2°.

## The field of vision

### Monocular field of view

On the temporal side, where there are no obstructions, the field of vision extends through more than 90° from the optical axis. The extreme ray entering the eye from this side follows approximately the path indicated in *Figure 2.13*. This diagram also explains why the retina extends so far forwards. It would not need to do so if light could not reach it.

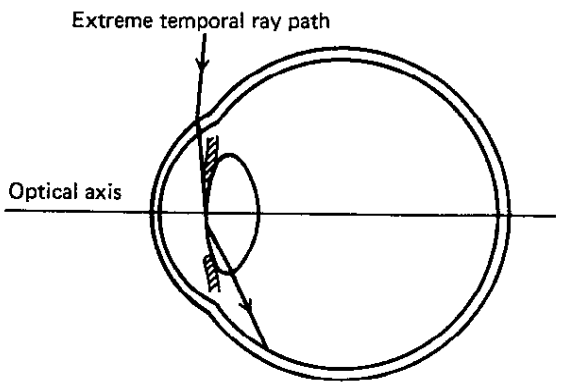


**Figure 2.13.** The ray path at the limit of the eye's field of view.

The nose, brow and cheek limit the monocular field of view in other directions, so that its shape is irregular. A more detailed treatment of the visual fields is given in Chapter 8.

One can note here a useful application of the nodal points. If UN and VN in *Figure 2.14* are incident rays enclosing an angle $u$, the conjugate refracted rays will diverge as though from N′, still including the same angle $u$. Suppose these rays meet the retina at U′ and V′. Then, without entering at all into questions of visual perception, one may draw the following inference: a linear extent of the retina subtending a known angle at the second nodal point corresponds to an equal angular extent of object space.

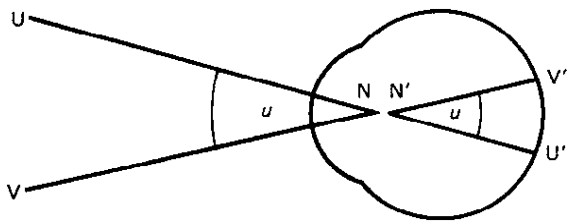


**Figure 2.14.** Visual projection through the nodal point.

The fovea is about 0.3 mm horizontally by 0.2 mm vertically, subtending an angle at the second nodal point of about 0.018 by 0.012 radians. At a typical reading distance of 350 mm, this would cover an area of 6.3 × 4.2 mm, wide enough for four letters of the size commonly used for newsprint.

### The blind spot

At the *papilla*, or optic disc, where the main trunk of the optic nerve leaves the eye, there are no retinal receptors. Consequently there is a corresponding 'blind spot' in the monocular field of vision, first noted by Mariotte in 1668.

The optic disc measures about 2 mm vertically by 1.5 mm horizontally, subtending an angle of some 7° by 5° at the second nodal point. This is also the angular subtense of the blind region in space. It has been pointed out that ten full moons placed side by side could disappear from view within this space.

The centre of the optic disc lies nasalwards from the fovea and slightly upwards from it. The centre of the blind space is accordingly some 15°

on the temporal side of the visual axis and 2° below it.

In *Figure 2.15*, the positions on the retina of the macula and optic disc are shown in relation to the posterior pole. Dimensions given in degrees refer to the angular subtense at the second nodal point.

Undoubtedly the most surprising feature of the blind spot is that normally its existence is never noticed. Even if one eye is occluded and the other views a strongly patterned or brightly coloured expanse, the observer is still not conscious of any gap. Nevertheless, the blind spot can easily be mapped if suitable fixation and moving test-objects are used.

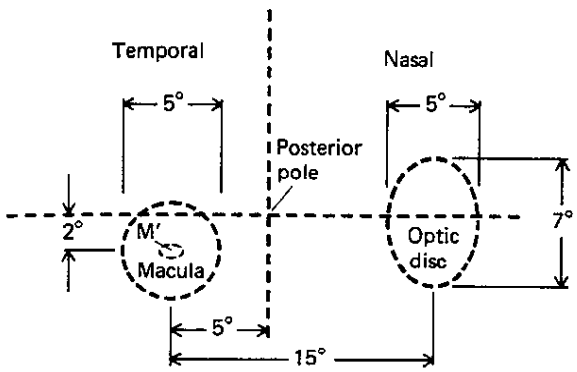


**Figure 2.15.** The relative sizes and positions of the macula and optic disc. M′ denotes the fovea.

Although the blind areas of the right and left eyes do not overlap, Bridgman (1964) has pointed out that in certain oblique directions of gaze part of the blind space of one eye is occluded by the nose from the field of vision of the other eye.

## The reduced eye

For most purposes, the optical imagery of the eye can be adequately studied on the basis of a simple analogue, called a 'reduced eye'. As shown in *Figure 2.16* it consists of a single convex surface separating air from a medium of refractive index $n'$ similar to that of the vitreous body.

Since convenience and simplicity are basic to the concept of a reduced eye, round figures are entirely appropriate. In Emsley's version, the power $F_e$ is taken as exactly +60 D and the value of $n'$ as 4/3. The two focal lengths, derived from equation (2.3) are

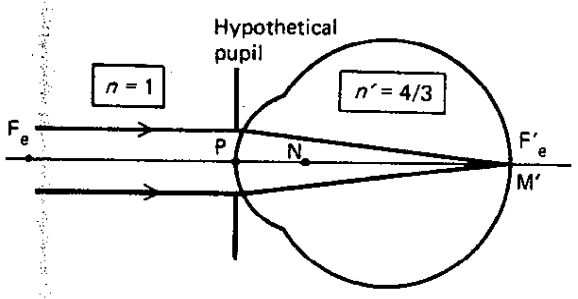


**Figure 2.16.** The reduced eye and its hypothetical pupil.

$$f_e = \mathrm{PF_e} = -1000/F_e = -1000/+60$$
$$= -16.67 \text{ mm}$$

and

$$f'_e = \mathrm{PF'_e} = 1000n'/F_e = \frac{4000}{3 \times 60}$$
$$= +22.22 \text{ mm}$$

In calculations it is often helpful to remember that these two focal lengths are exactly −50/3 and +200/9 mm respectively.

Equation (2.3) also gives the necessary radius of curvature $r$ of the refracting surface as

$$r = \frac{1000\ (n' - 1)}{F_e} = \frac{1000}{3 \times 60} = +5.56 \text{ mm}$$

As a vulgar fraction, this is exactly 50/9 mm.

In the case of a single refracting surface, the two principal points coincide with each other and with the vertex of the surface, denoted by P. Similarly, the two nodal points coincide with each other and with the centre of curvature of the surface (now denoted by N). This is logical, since any ray directed toward this point meets the surface normally and is hence undeviated.

The line passing through P and N constitutes the optical axis, and the fovea, denoted by M′, is assumed to be on this line which accordingly becomes the visual axis as well.

If the unaccommodated eye is in focus for distant objects it is said to be 'emmetropic'. In this event its second principal focus F′ coincides with M′.

For convenience, the pupil of the reduced eye is considered to lie at the refracting surface, as shown in *Figure 2.16*. The entrance and exit pupils now coincide with this hypothetical pupil and the principal point P fills the additional role of being the centre of the pupil.

*Figure 2.17* sets in juxtaposition the reduced and the Gullstrand–Emsley schematic eye with the second principal focus F′ of each in coincidence.

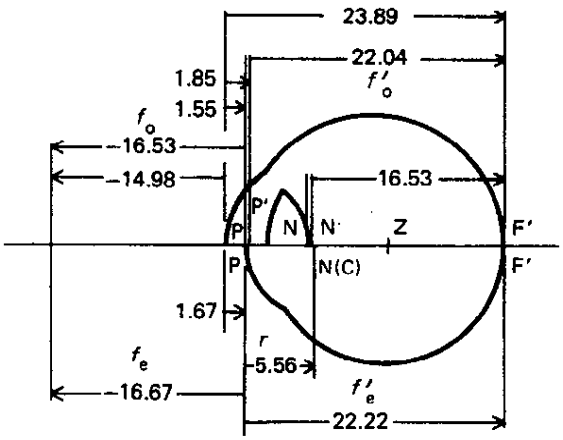


**Figure 2.17.** Comparison of the Gullstrand–Emsley schematic eye with the simple reduced eye.

The principal point of the reduced eye is seen to lie in between the two principal points of the schematic eye. In round figures, the vertex of the reduced eye lies 1⅔ mm behind that of the schematic eye. Hence, if a spectacle lens is assumed to be 12 mm from the cornea, its distance from the reduced eye should be reckoned as 13⅔ mm.

## The retinal image

### Algebraic treatment

The retinal image is inverted – a fact first propounded by Kepler in the early seventeenth century and later demonstrated by Scheiner.

A distinction must be drawn between the retinal image, which may be sharp or blurred according to circumstances, and the optical image. This latter term denotes the sharp image formed by the refracting system of the eye as though the retina were absent. The actual formation of the optical image is, of course, prevented if it lies behind the retina.

Given the necessary data, the position and size of an optical image can be determined from the algebraic formulae already given in this chapter.

***Example 1***

An object 50 mm high is situated on the optical axis of the standard emmetropic reduced eye at a distance of 250 mm from its principal point. Find the position and size of the optical image.

It is easier to work in terms of vergences. Thus

$$\ell = -250 \text{ mm}$$
$$L = 1000/-250 = -4.00 \text{ D}$$
$$F_e = +60.00 \text{ D}$$
$$L' = L + F_e = +56.00 \text{ D}$$
$$\ell' = 1000n'/L' = \frac{4000}{3 \times 56} = +23.81 \text{ mm}$$

The height $h'$ of the optical image can be found from equation (2.10)

$$h' = hL/L' = \frac{50 \times -4.00}{+56.00} = -3.57 \text{ mm}$$

The minus sign denotes inversion of the image.

Since the image distance in this case (23.81 mm) is greater than the axial length of the eye (22.22 mm), the optical image becomes a theoretical construction only.

### Object at infinity

An object at infinity is imaged in the plane of the second principal focus. Its size depends on the angular subtense of the object.

In *Figure 2.18*, rays from the extremity Q of a distant object inclined at the positive angle $u$ to the optical axis are focused at Q′ in the plane of $F'_e$. A ray through the nodal point is undeviated. A ray incident at P is deviated towards the axis, the refracted ray making an angle $u'$ with it such that

$$n' \sin u' = n \sin u$$

in accordance with the law of refraction.

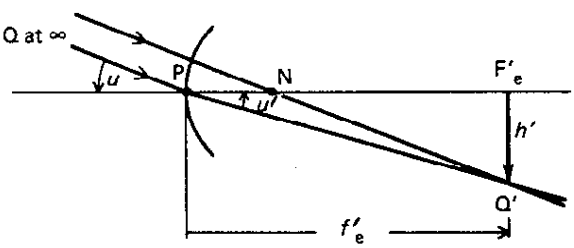


**Figure 2.18.** Image construction in the reduced eye: distant object.

the last expression can be put in the simpler paraxial form

$$n'u' = nu = u \qquad (2.15)$$

or

$$u' = u/n' \qquad (2.16)$$

From the diagram

$$u' = -h'/f'_e$$

and thus

$$h' = -u'f'_e = -uf'_e/n' = -u/F_e \qquad (2.17)$$

In this expression, $h'$ is in metres and $u$ in radians.

***Example 2***

A distant object subtending an angle of 5° is viewed by a reduced eye with a power of +62 D. Find the position and size of the optical image.

$$\ell' = f'_e = n'/F_e = \frac{4000}{3 \times 62} = +21.51 \text{ mm}$$

$$u = 5 \times \pi/180 = 0.0873 \text{ rad}$$

$$h' = \frac{-0.0873 \times 1000}{62} = -1.41 \text{ mm}$$

**Ray-construction methods**

The image formed by a single refracting surface such as the reduced eye can be found by constructing two or more ray paths from the given object point.

Diagrams of this kind are drawn to scale, but different scales may be used for horizontal and vertical dimensions. The refracting surface should be replaced by the tangent to its vertex.

The ray paths commonly used in these constructions are shown in *Figure 2.19*, in which BQ is an object for the eye. The image point Q′ is the intersection of any two (or more) of the following refracted rays originating from Q.

Ray 1 Parallel to the optical axis, passing through $F'_e$ after refraction.
Ray 2 Through the first principal focus $F_e$, refracted parallel to the axis.
Ray 3 Through the nodal point, undeviated.
Ray 4 Directed towards the principal point P.

To find the refracted ray path for this last ray, locate the point Y on BQ such that

$$BY = BQ/n' = 0.75\ BQ$$

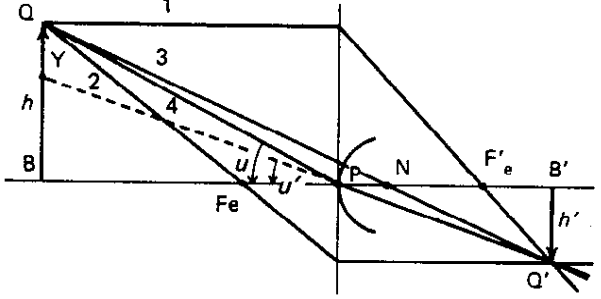


**Figure 2.19.** Image construction in the reduced eye: near object.

The refracted ray path is YP produced. This construction is justified by equation (2.16) which can be written as

$$\tan u' = (\tan u)/n'$$

since it has already been assumed that $u$ is small.

It can be most useful to carry out constructions of this kind, verifying the results by calculation. However, it should be borne in mind that they are subject to the same limitations as the approximate expressions on which they are based.

## Nature of mirror imagery

The so-called lateral inversion of the image formed by a plane mirror, notably one's own reflection, still gives rise to perplexity and debate. Arguments from psychological or related grounds tend to be needlessly invoked.

To understand the true nature of mirror imagery demands consideration of an object in three dimensions, not two. For a plane mirror, any object point and its reflected image lie on a common normal to the surface and are equidistant from it. Consequently, the object shown in *Figure 2.20*, representing a central vertical section through the head of an observer, is imaged as depicted. The image is formed as though the object had been pulled through the mirror, and turned inside out in the process. The same would take place in any vertical section parallel to the plane of the diagram. As a result, the left eye of the observer appears as the right eye of the three-dimensional image gazing back at him.

Just as a right-hand glove turned inside out takes the form of a left-hand glove, so the mirror

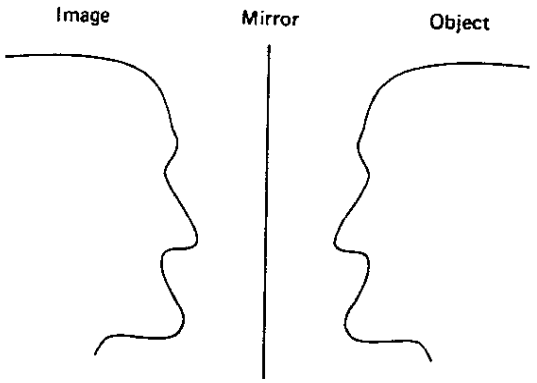


**Figure 2.20.** Vertical section through the centre of an observer's head and its mirror image. Since imagery of the same type takes place in every plane parallel to that of the diagram, it follows that the left eye of the observer becomes the right eye of the three-dimensional mirror image, and *vice-versa*.

image of one's own right hand apears as a left hand. The same three-dimensional transformation is shown by the virtual images formed by concave and convex mirrors, accompanied by magnification or its opposite.

Clearly, the term 'lateral inversion' does not adequtely describe the phenomenon. 'Mirror metamorphosis' is offered as an improvement on the term 'perversion', which has been suggested in the past without gaining effective support.

## Exercises

**2.1** (a) A pencil of rays emerges from a lens with a vergence of +6.00 D. What is its vergence after a travel of 10 mm in air? (b) A pencil of rays emerges from a lens with a vergence of −8.00 D. What is its vergence after a travel of 15 mm in air?

**2.2** The macula of an emmetropic reduced eye has a diameter of 1.5 mm. What angle does it subtend at the nodal point and what is the corresponding linear extent of object space at 10 m from the eye?

**2.3** A schematic eye has a single-surface cornea of 7.5 mm radius of curvature, an anterior chamber depth of 3 mm and a homogeneous crystalline lens of thickness 3.5 mm, refractive index 1.4 and back surface radius of curvature −6 mm. Both aqueous and vitreous have a refractive index of 1.336. Calculate the position and magnification of the entrance and exit pupils.

**2.4** The diagram, (not to scale) illustrates the positions P and P′ of the principal points of a telephoto lens system formed by two thin lenses of power +10 D and −5 D at $A_1$ and $A_2$ respectively. An object point B and its image B′ are also shown. From the given measurements, all in mm, determine the following distances, using in each case only distances of stated length and paying strict attention to signs: $A_1P$, $A_2F'$, PP′, F′B′ and PB. (Example: $FB = FA_1 + A_1B = -(-162.5) + (-662.5) = -500$ mm.)

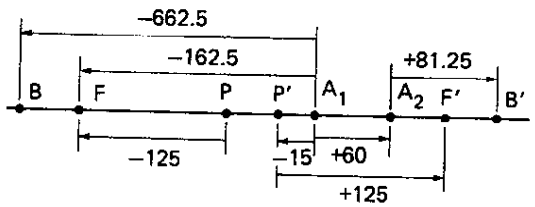


**2.5** The diagram illustrates a diverging meniscus lens of thickness $t$ with its first principal point P at a distance $e$ from vertex $A_1$ and its second principal point P′ at a distance $e'$ from vertex $A_2$. An object point B is at a distance $\ell$ from P and its image B′ at a distance $\ell'$ from P′. Using only these letter symbols, express the following distances: $P'A_1$, $A_2B'$, PP′, B′P and BB′. (Example: $A_1B = A_1P + PB = e + \ell$.)

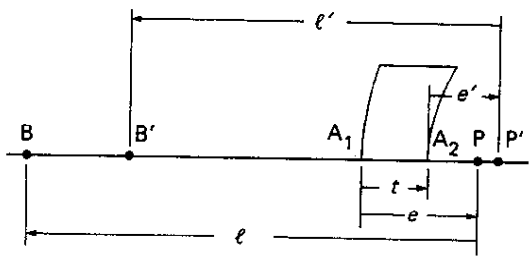


## References

BRIDGMAN, C. S. (1964) Viewing conditions under which the blind spot is not compensated by vision in the other eye. *Am. J. Optom.* **41**, 426–428

IVANOFF, A. (1953). *Les Aberrations de l'Oeil*. Paris: Editions de la Revue d'Optique

PRENTICE, C. F (1890). A metric system of numbering and measuring prisms. *Archs Ophthal., N.Y.* **19**, 64–75, 128–135

WOOD, R. W. (1911). *Physical Optics*, 2nd edn. New York: Macmillan

registrations show an even greater proportion in the 70 plus age group.

Patients whose near acuity is N12 or lower and wish to become members of the Talking Book Service of the Royal National Institute for the Blind can have their application form signed by an optometrist. They may have to pay the annual subscription themselves.

In the United Kingdom, registered blind people are eligible for various concessions including an increased tax allowance and, if necessary, higher rates of supplementary benefit. Braille and Moon embossed-type books and tape-recorded books are available on loan, while local authorities can provide welfare services.

In the latest of a series of official reports on blindness (Department of Health and Social Security, 1979), the incidence, degree and causes of blindness in England were shown to be broadly similar in the two sexes. Among children, the major causes are congenital anomalies, optic nerve atrophy and cataract. The two latter conditions, together with choroidal atrophy, glaucoma, diabetes, retinitis pigmentosa and other retinal conditions, are the main causes of blindness in adults.

A further Report by the Department was published in 1988, presenting statistics for 1976/77 and 1980/81. Though there has been little change in the annual number of new registrations, the increasing life span is reflected in the fact that the age group 75 and over constitutes a growing percentage of the total of the registered blind. In the four years separating the two periods studied, the percentage rose from 54.1 to 58.6 per cent. In this most elderly group, retinal degenerative conditions are the largest single cause of blindness.

Among adults up to 64 years old, diabetic retinopathy is the largest single cause. A point of particular interest is the marked increase in the proportion of women to men who become blind for this reason within the age group 55 to 64.

A more detailed study of this Report has been made by Giltrow-Tyler (1988).

In the USA, a typical definition of blindness is that 'a person shall be considered blind who has a visual acuity of 20/200 or less in the better eye with proper correction, or limitation in the field of vision such that the widest diameter of the visual field subtends an angular distance no greater than 20°'. This definition may vary in different States. According to the amended AMA visual efficiency ratings published in 1955, a person would be considered blind if his binocular visual efficiency was below 10%.

Statistics and clinical data on blindness in the USA are compiled by a Model Reporting Area on Blindness Statistics. This is a voluntary association of States having uniform definitions and procedures for that purpose. Publication of reports is undertaken by the US Department of Health, Education and Welfare.

There is no British legal definition of partial sight, but registration is normally open to those whose visual acuity is:

(1) from 3/60 to 6/60 with full visual field,
(2) up to 6/24 with moderate contraction of the field, opacities in the media or aphakia,
(3) 6/18 or better if there is a gross field defect.

Children with acuities between 3/60 and 6/24 may be taught in special schools for the partially sighted, but a child with acuity better than 6/24 will usually be taught in a normal school.

In England, about 0.1% of the population are registered as partially sighted but the number eligible for registration is thought to be considerably more than this. The main reason is that registration carries no entitlement to the tax and certain other of the concessions available to the blind. The age distribution of the registered partially sighted in England is similar to that of the registered blind. New registrations account for about one-fifth of the total annually.

## Modulation transfer function and the eye

### The sinusoidal grating

Conventional clinical assessments of visual acuity are related to the eye's resolving power. Another method of assessment is based on the eye's sensitivity to luminance contrast. Although 'square wave' or Foucault gratings could be used for this purpose, sinusoidal gratings (*Figure 3.23*) are preferred. The name arises from the fact that a continuous plot of the luminance along a perpendicular to the bars would represent the function

$$y = a\sin(bx) + c$$

An important advantage of this type of grating is that even when defocused or affected by aberrations, its image generally retains the sinusoidal luminance pattern.

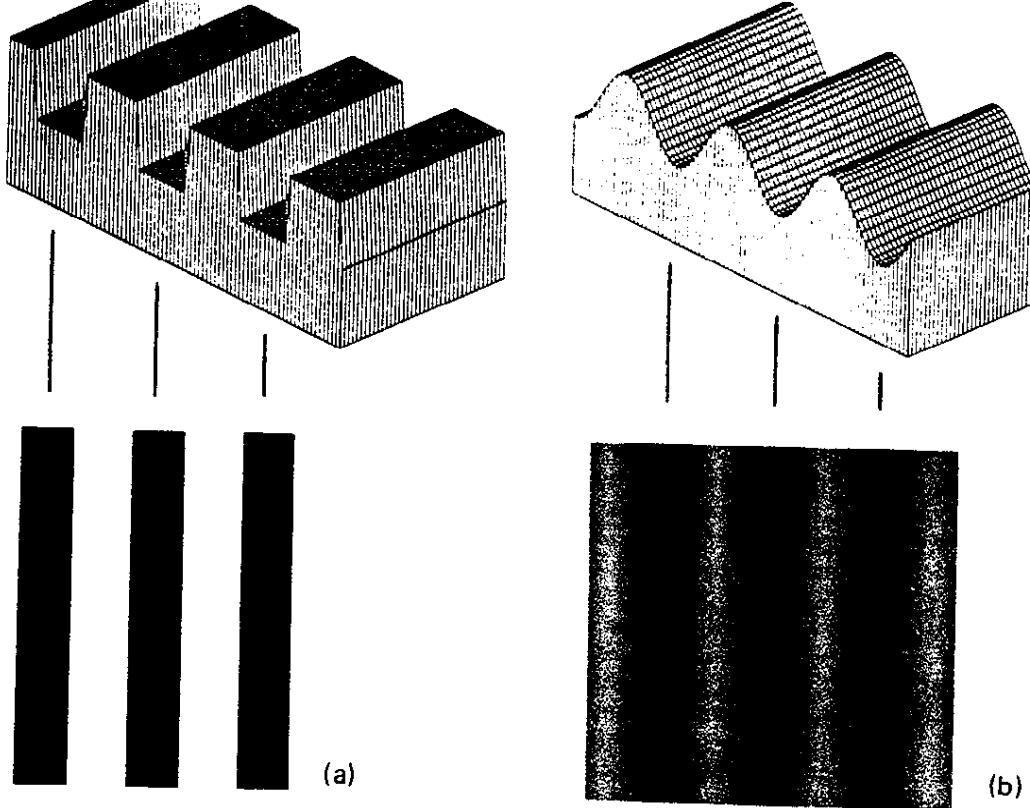


**Figure 3.23.** (a) A square-wave or Foucault grating. (b) A sinusoidal grating of the same frequency. The upper drawings show corresponding three-dimensional representations of the spatial luminance profile. (Material for this illustration kindly provided by Dr J. Barbur.)

Basic definitions may be understood by reference to *Figure 3.24* which shows the luminance curves of two sinusoidal gratings having the same mean luminance and cycle width.

If $L_{min}$ is the minimum and $L_{max}$ the maximum luminance, then

$$\text{Modulation} = \frac{L_{max} - L_{min}}{L_{max} + L_{min}} \qquad (3.16)$$

*Table 3.4* gives the values of $L_{max}$, $L_{min}$ and the modulation for the two curves illustrated in *Figure 3.24*.

**Table 3.4** Values for luminance curves A and B in *Figure 3.24*

| *Curve* | $L_{min}$ | $L_{max}$ | *Mean luminance* | *Modulation* |
|---|---|---|---|---|
| A | 0 | 80 | 40 | 1 |
| B | 30 | 50 | 40 | 0.25 |

The modulation can be regarded as the maximum change in luminance from its mean value, expressed as a ratio of this value. When the minimum luminance is zero, as in curve A, the modulation is equal to unity.

In the literature of contrast sensitivity, the term 'contrast' has come into general use to denote a

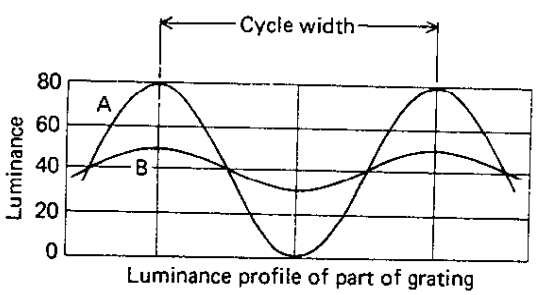


**Figure 3.24.** Sinusoidal grating: luminance profile. Curve A has greater modulation than curve B.

numerical value of modulation as defined by equation (3.16). It is usually expressed as a percentage. For purposes of comparison, this same definition of contrast is sometimes applied to test charts of both high and low contrast. In other contexts including standardization, the contrast of a test chart is defined differently as noted earlier (*see* page 41).

The cycle width of a sinusoidal grating corresponds to the 'grating interval' of a square grating, but is usually expressed as a spatial frequency. Thus, if the cycle width subtends an angle of $\theta$ degrees at the observer's eye,

$$\text{Spatial frequency } \nu = 1/\theta \text{ cycles/degree}$$

For example, 60 cycles/degree corresponds to a cycle width subtending 1 minute of arc. Gratings used as test objects do not necessarily have a uniform spatial frequency. For some purposes it may vary in a definable manner, such as logarithmically.

If a sinusoidal grating is presented to the eye, its threshold of recognition as a grating is affected both by its spatial frequency and its luminance contrast.* As the contrast is reduced, recognition becomes harder as with other test objects. Moreover, with high spatial frequencies the loss of contrast in the retinal image is greater than with low frequencies, again making recognition more difficult.

In numerical terms, contrast sensitivity at a given spatial frequency is the reciprocal of the threshold value of the modulation as defined by equation (3.16). It is a measure of the eye's ability to detect small differences in luminance.

For example, if a grating can just be resolved when the modulation has been reduced to 0.08, the contrast sensitivity is 12.5. If the threshold modulation had been at the lower figure of 0.02, the contrast sensitivity would have risen to 50. This higher value indicates a superior performance.

## The modulation transfer function

When a sinusoidal grating is imaged by an optical system, the contrast of the image is reduced by the effects of aberrations and diffraction. Nevertheless, it retains the sinusoidal luminance pattern, though with a lowered modulation. In general, the ratio of the modulation of the image of a grating of given spatial frequency to that of the object is called the modulation transfer factor. A plot of this transfer factor against spatial frequency depicts the modulation transfer function (MTF). It provides a good indication of the performance of the image-forming system at varying frequencies, not just the finest.

Modulation transfer functions for the optical system of the human eye were obtained from a two-stage experimental process by Campbell and Green (1965a). In brief, their method was to form sinusoidal interference fringes on the retina by an adaptation of Young's double-slit system (*see also* page 52). In this arrangement, the angular separation $\theta$ between successive bright fringes is given by

$$\theta \text{ (rad)} = (\lambda/a) \times 10^{-6} \qquad (3.17)$$

where $\lambda$ is the wavelength (in nm) of the monochromatic light source used (632.8 nm in this experiment) and $a$ (in nm) the separation of the slits. To vary the contrast of the interference pattern, the source producing it was dimmed. At the same time, the mean retinal illuminance was kept constant by the addition of a uniform field of light of the same wavelength. Since the interference fringes are not affected by the eye's optics, measurement of the threshold modulation as a function of spatial frequency gives the contrast sensitivity of the retina and neural system alone.

To provide a comparable test object viewed directly by the entire visual system, including the degrading effects of the ocular dioptrics, a sinusoidal grating was generated by means of an oscilloscope with a spectral luminance peak at 530 nm. The performance of the eye was considered not to vary significantly between wavelengths of 530 and 632.8 nm if the luminance were the same. The contrast sensitivity was determined over the same range of variables as before. For the same observer with a 2 mm pupil, the results are shown by the lower curve in *Figure 3.25*. Since the actual contrast in the retinal image at the threshold of recognition can be assumed to be the same in both cases, the reduced contrast sensitivity for the grating imaged by the eye can only be due to the defects and limitations of the eye's optical system with a pupil diameter of

* In this context, the term luminance contrast has come to be used as a synonym for modulation in its quantitative sense.

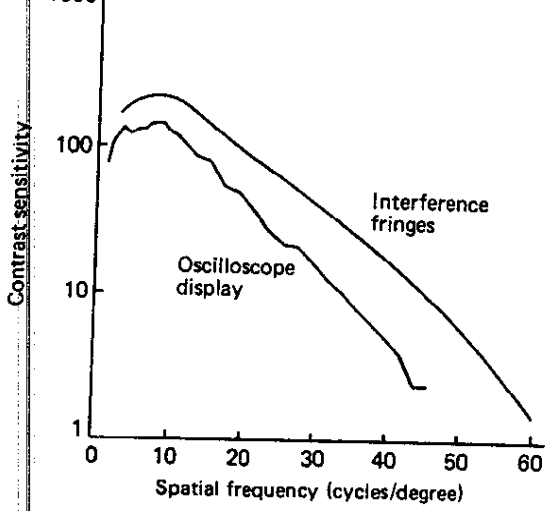


**Figure 3.25.** Contrast sensitivity of the human eye. Upper curve: measurements obtained from interference fringes, assessing retinal/neural function; lower curve: measurements obtained from an oscilloscope display, assessing optical as well as retinal/neural factors. (Redrawn from Campbell and Green, 1965a by kind permission of the publishers of *J. Physiol.*)

2 mm. The oscilloscope observations can be repeated with other pupil diameters.

For a spatial frequency of 1 cycle/degree, a sinusoidal grating viewed at 40 cm would need to have a cycle width of 7.0 mm. As suggested by *Figures 3.25 and 3.26* and confirmed by other results, the spatial frequency for which the contrast sensitivity is greatest is about 3 cycles/degree for a typical observer. A limiting frequency of 30 cycles/degree, corresponding to a cycle width of 2 minutes, would conventionally be equated to an acuity of 6/6 (20/20), at least for a square-wave grating.

A modulation transfer function can be plotted from the data of *Figure 3.25.* Because contrast sensitivity is the reciprocal of modulation, it follows that the modulation transfer factor is the inverse ratio of the sensitivity for the interference fringes to that for the oscilloscope display. For example, at a spatial frequency of 10 cycles/degree the two values are approximately 206 and 128, giving a transfer factor of 128/206 or 0.62. At 40 cycles/degree the values are approximately 17.5 and 4.9, the transfer factor being 0.28.

The complete graph of the modulation transfer function for this pupil diameter is shown in *Figure 3.27*, together with the curves for pupil diameters

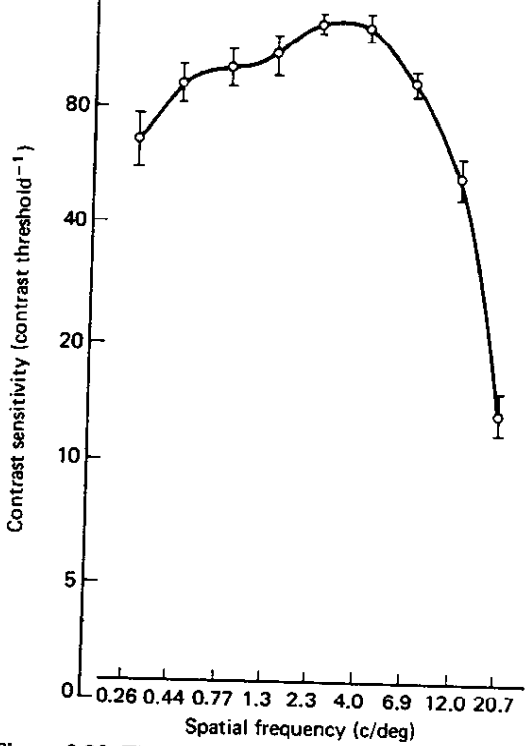


**Figure 3.26.** The contrast sensitivity function (mean of measurements on ten normal subjects aged between 18 and 27 years). The bar lines represent ±1 standard error. Note that both scales are logarithmic. (Reproduced from Wright and Drasdo (1985), by kind permission of the publishers of *Documenta Ophthalmologica* and reprinted by permission of Kluwer Academic Publishers.)

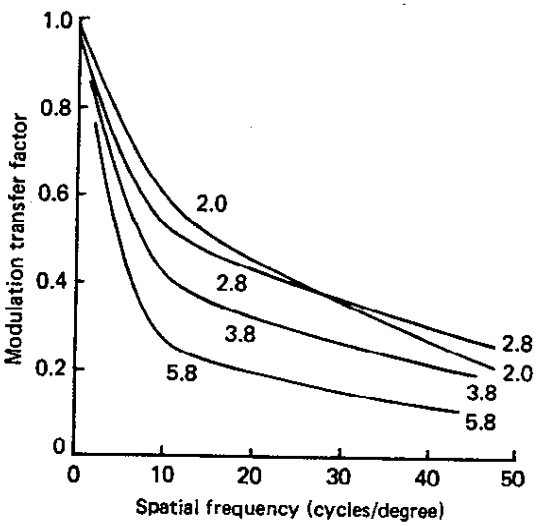


**Figure 3.27.** Modulation transfer function for a human eye at various pupil diameters. (Reproduced from Campbell and Green, 1965a by kind permission of the publishers of *J. Physiol.*)

of 2.8, 3.8 and 5.8 mm, all for the same subject. It can be seen that the curves for 2 and 2.8 mm pupils are not only very close together, but actually cross over at about 27 cycles/degree. On this evidence, the eye's performance changes little within this range of pupil diameters – a result confirmed by the lightly curved top of the acuity/pupil diameter graph of *Figure 3.6*.

Campbell and Green (1965b) showed that the contrast sensitivity measured binocularly was approximately 40% better than that found under monocular conditions over a wide range of frequencies. They attributed this to the summation of signals from the two eyes.

### Normalized spatial frequency

If an eye of pupil diameter $g$ had a perfect optical system limited only by diffraction, the minimum angle of resolution $\theta_{min}$ for two point sources would be

$$\theta_{min}\,(\text{rad}) = 1.22\lambda/g \qquad (3.2)$$

For a sinusoidal grating, with $\theta_{min}$ the smallest angular cycle width which can be resolved, the corresponding relationship is

$$\theta_{min} = \lambda/g\ (\text{rad})$$
$$= 57.3\lambda/g\ (\text{degrees}) \qquad (3.18)$$

The maximum spatial frequency ($\nu_{max}$) which can be discerned – the 'cut-off point' – is thus

$$\nu_{max} = 1/\theta_{min}$$
$$= g/57.3\lambda\ (\text{cycles/degree}) \qquad (3.19)$$

For example, given $g = 3$ mm and $\lambda = 560$ nm

$$\nu_{max} = 3 \times 10^{-3}/(57.3 \times 560 \times 10^{-9})$$
$$= 93.5\ \text{cycles/degree}$$

To facilitate comparison between the MTF of an actual eye and that of a diffraction-limited eye, the concept of normalized spatial frequency is used. Irrespective of pupil diameter and wavelength, the cut-off frequency $\nu_{max}$ for the diffraction limited eye is fixed at unity. On this normalized scale, any actual value of $\nu$ is replaced by the normalized value $\nu_n$ such that

$$\nu_n = \nu/\nu_{max}$$

From equation (3.19) it follows that

$$\nu_n = (57.3\lambda/g)\nu \qquad (3.20)$$

with $\nu_n$ and $\nu$ both in cycles/degree.

In this way a single MTF curve can be used to represent any diffraction-limited optical system, irrespective of particular values of $g$ and $\lambda$.

The complete MTF for a diffraction-limited eye or optical system can be calculated by standard mathematical procedures (Westheimer, 1972a). If the pupil were rectangular in shape, with its narrower width $g$ perpendicular to the grating bars, the MTF graph would be a straight line as shown in *Figure 3.28*. For a circular pupil, the graph assumes the shape indicated in the diagram. The cut-off point is the same for both.

In *Figure 3.29*, the MTF curves of *Figure 3.27* are shown re-plotted on a normalized frequency scale. This process could have been carried out by

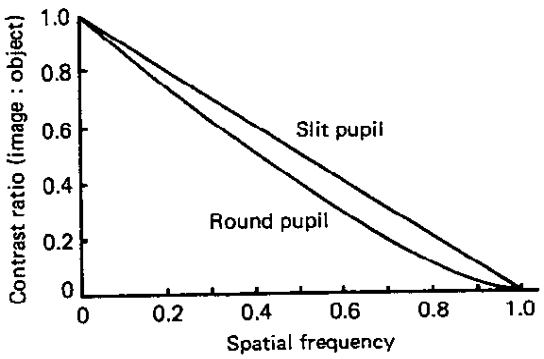


**Figure 3.28.** The modulation transfer function for a diffraction-limited eye or system with a slit and a round pupil. (Reproduced from Westheimer, 1972 by kind permission of the publishers. Springer, Berlin and New York.)

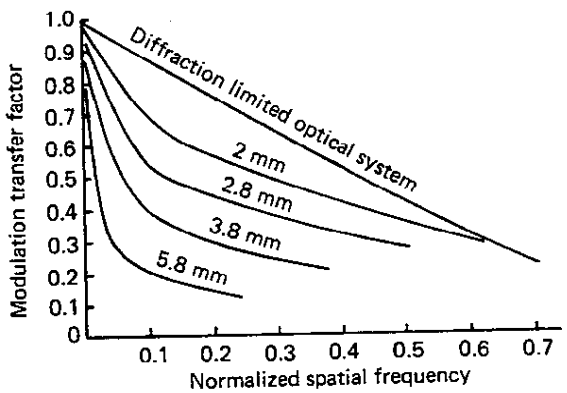


**Figure 3.29.** The modulation transfer function of a human eye plotted for a normalized spatial frequency. (Reproduced from Campbell and Green, 1965a by kind permission of the publishers of *J. Physiol.*)

using equation (3.20). For example, the end point of the graph for 5.8 mm pupil size in *Figure 3.27* occurs at an actual frequency of about 45 cycles/degree, the wavelength being 530 nm. Accordingly,

$$\nu_n = \frac{57.3 \times 530 \times 10^{-9}}{5.8 \times 10^{-3}} \times 45 = 0.24$$

which agrees with *Figure 3.29*. If continued, the graph representing the diffraction-limited system would meet the $x$-axis at the cut-off point where $\nu_n = 1$.

The curves in *Figure 3.29* for various pupil diameters of the same eye should not be compared with each other, but only with the theoretical comparison curve. The diffraction-limited eye performs better as its pupil diameter increases and so becomes a harder standard of comparison.

## The double-pass technique

The double-pass technique requires only one set of experimental results from which to compute the MTF of an eye. It has been used in many investigations. In the arrangement described by Campbell and Gubisch (1966), the image of a narrow illuminated slit is formed on the fundus. Acting as a diffusing surface, the fundus reflects a portion of the incident light back through the pupil. It then passes through a beam-splitter and a converging lens which forms an aerial image of the fundus streak. This can be examined either photographically or photo-electrically, allowance being made for the effects of the reverse passage through the optical media. Analysis of the light distribution in the streak image enables the line-spread function of the eye's optical system to be determined. Its graph resembles a Gaussian normal distribution curve. By a mathematical process known as Fourier analysis, the modulation transfer function can be computed from the line-spread function. In this context, Fourier's more general theorem shows that the light distribution across a narrow slit or its image can be resolved into an infinite series of sine waves of increasing frequency.

The conventional index of the narrowness of a Gaussian-type curve is its 'half-width' – the width at half the peak value. Graphs of the image line-spread for one of Campbell and Gubisch's subject's showed the half-width to decrease with pupil size: from 6.2 minutes of arc at 6.6 mm pupil diameter to 2.2 minutes at 2.4 mm pupil diameter. For smaller pupil sizes, the half-width increased, reaching 3.2 minutes with a 1.0 mm pupil. Over this range, the reduction in the eye's aberrations becomes increasingly outweighed by the effects of diffraction.

The MTF graphs obtained by Campbell and Gubisch for their three subjects are broadly similar to the results of Campbell and Green (1965a). For two of their subjects the curves for 2.0 and 3.0 mm pupils cross over as in *Figure 3.27*.

## Square-wave (Foucault) gratings

Unlike sinusoidal ones, square-wave gratings are easily produced without special equipment, making them useful experimentally. According to Fourier analysis, a square wave of frequency $\nu$ and amplitude $a$, denoting $\frac{1}{2}(L_{max} - L_{min})$, is equivalent to a sine wave of the same frequency $\nu$ but of amplitude $4a/\pi$ plus a series of sine waves of increasing frequency and decreasing amplitude. Each wave, including the first, is called a harmonic. The $n$th harmonic has the frequency $n\nu$ and amplitude $4a/\pi n$, but in this series only the odd-numbered values of $n$ are included, as shown in *Table 3.5*.

**Table 3.5** Frequency and amplitude of odd-numbered harmonics

| *Harmonic* | *Frequency* | *Amplitude* |
|---|---|---|
| First | $\nu$ | $4a/\pi$ |
| Third | $3\nu$ | $4a/3\pi$ |
| Fifth | $5\nu$ | $4a/5\pi$ |
| . | . | . |
| . | . | . |
| . | . | . |

The bold lines in *Figure 3.30* show one half of a square wave of amplitude $a$ and the corresponding half of the first harmonic of the equivalent sine-wave series. The lower part of the diagram shows the third and fifth harmonics. Curves representing the sum of the first and third, and the sum of the first, third and fifth harmonics are also displayed. It can be seen that even though these curves still oscillate, they steadily approach the outline of the square wave.

If the third and subsequent harmonics are ignored, a square-wave grating can be regarded

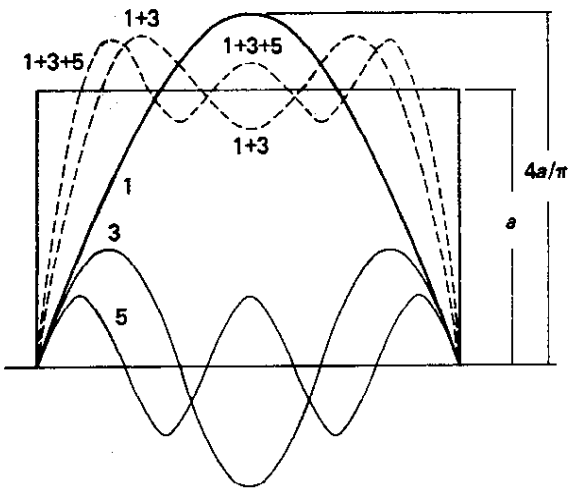


**Figure 3.30.** Partial generation of a square wave by compounding sine waves of frequencies of the first, third and fifth harmonics.

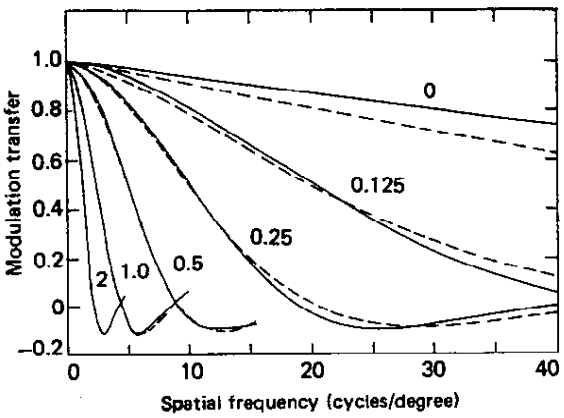


**Figure 3.31.** Variation in the modulation transfer function with defocus for an aberration-free eye with a 5 mm diameter entrance pupil, according to physical optics. The solid curves show the MTFs at 450 nm, the broken curves the MTFs at 650 nm, for both positive and negative errors of focus of the amounts indicated in dioptres. There is very little difference between the MTFs at the two wavelengths when the errors of focus are large. (Reproduced from Charman and Jennings, 1976 by kind permission of the publishers of *Br. J. Physiol. Optics.*)

as a sinusoidal grating of the same spatial frequency but of $\pi/4$ times the amplitude. It then follows that the contrast sensitivity thresholds for square-wave and sinusoidal gratings of the same frequency *and* amplitude should in theory be in the ratio of $4/\pi$.

Since the frequencies of the subsequent harmonics are multiples of the basic frequency (of the first harmonic), they could all be situated beyond the cut-off point. For this reason alone it is evident that they can become significant only when the basic frequency lies within a restricted range. The limits of this range were explored by Campbell and Robson (1968) by determining the contrast sensitivity thresholds for square and sinusoidal gratings of the same frequency and amplitude. The expected ratio of $4/\pi$ was found to hold good for gratings of spatial frequency exceeding 0.8 cycles/degree. At lower frequencies, the ratio increased rapidly, probably due to selective response by individual neural elements in the visual system to particular frequencies.

## Effects of defocus and spurious resolution

All the MTF results described above have assumed the eye to be in focus for the grating. When it is out of focus, the theory of both geometrical and physical optics predicts that modulation transfer suffers appreciably, even for very small errors. This is shown in *Figure 3.31* (Charman and Jennings, 1976), which refers to the theoretical diffraction-limited eye with a 5 mm pupil. Even with an error as small as 0.12 D, the modulation falls much more rapidly with increasing spatial frequency than in the perfect eye. As the image modulation in the defocused eye drops to zero, it falls below the threshold for detection. The grating can no longer be resolved but assumes a uniform grey appearance.

At spatial frequencies greater than this threshold value, a phenomenon known as spurious resolution may occur. A simple explanation in general terms can be given with reference to a Foucault grating of relatively low spatial frequency. The effects of diffraction can then be ignored, being negligible in relation to those of geometrical out-of-focus blurring.

In *Figure 3.32*, the lines AB, CB, etc. represent the dark bars of a Foucault grating, equal in width to the white bars. If BC is taken to be a luminous line, the cross-section of a white bar, its blurred image consists of a succession of overlapping blur circles of diameter $j$ and its overall length JK is equal to (BC + $j$). When the bar width is greater than $j$, as in *Figure 3.32(a)*, the blurred images of the white bars are well separated and in register with the actual white bars.

An essential part of this explanation is that the luminance of the blurred image of any white bar

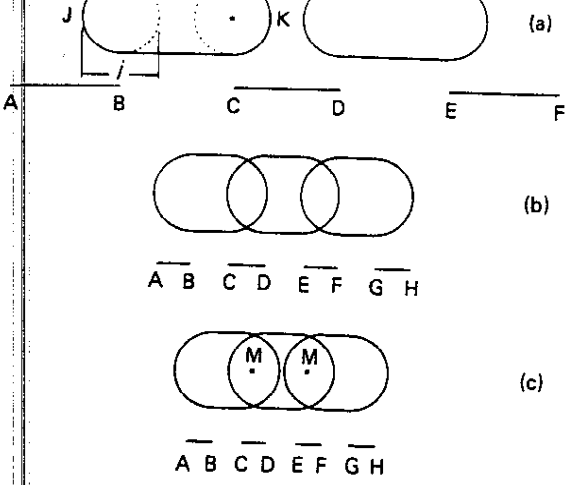


**Figure 3.32.** Spurious resolution: an explanation based on geometrical optics.

such as BC is not uniform along its centre line JK but tapers off identically at each end.

As the bar width decreases with $j$ remaining constant, the successive blurred images begin to overlap as in *Figure 3.32(b)*. For one particular bar width, the overlap of the two end portions of diminishing relative luminance is such that their combined luminance visually matches that of the surrounding areas. This condition occurs when the bar width is approximately equal to $j/2$.

At first sight this would appear to indicate the cut-off spatial frequency of the grating for the given degree of blurring. If, however, the bar width is further decreased beyond this point, as in *Figure 3.32(c)*, the areas of overlap become larger. The sum of the two separate luminances then reaches a peak at the midpoint M of the overlap area, higher than that in the area surrounding the overlap. A periodic pattern thus re-emerges visually, giving rise to 'spurious resolution'. However, since the luminous peaks at M are situated at the centre of the black bars of the grating, a black/white reversal has occurred.

As the bar width continues to be reduced, a second point is reached where the luminance across the grating is apparently uniform. This occurs when the bar width is approximately $j/4$. Spurious resolution also re-occurs as the bar width continues to decrease and further similar sequences are possible, though not necessarily discernible.

These appearances can best be observed in a radial grating, such as *Figure 3.33*, which gives increasing spatial frequency towards its centre. Grey annuli separating zones of successive contrast reversal or discontinuity can be seen if the grating is held close to the eye with the accommodation relaxed.

In *Figure 3.31*, contrast reversal of spurious resolution occurs when the modulation transfer factor assumes a negative value. These graphs, calculated on the basis of physical optics, give a more reliable picture than computations based on geometrical optics. Nevertheless, as shown by Charman and Jennings, the differences are negligible when the defocus error exceeds 0.50 D.

A detailed theoretical analysis of spurious resolution has been given by Smith (1982a). One of his conclusions is that spurious resolution is unlikely to be visible when the spatial frequency exceeds about 35 cycles/degree.

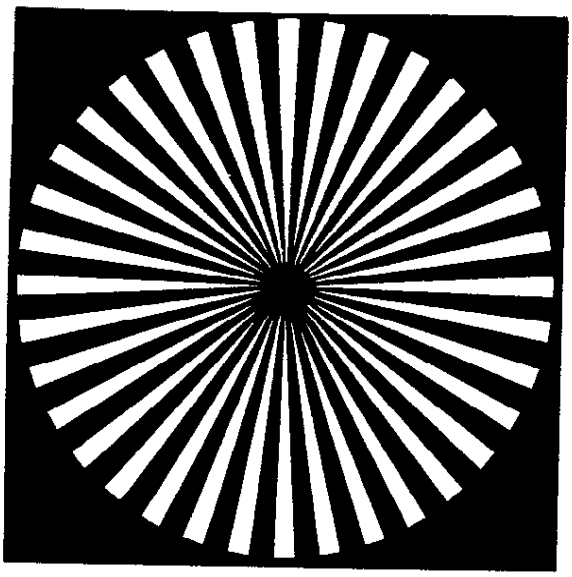

**Figure 3.33.** Radial square-wave grating to demonstrate unresolved annuli and zones of spurious resolution when held close to the eye and viewed out of focus.

## Contrast sensitivity

### Clinical considerations

Contrast sensitivity testing is normally undertaken at photopic luminances. The results of Van Nes and Bouman (1967), *Figure 3.34*, show a